Luminescence of Tris(2,2′-bipyridine)ruthenium(II) Cations ($[Ru(bpy)_3]^{2+}$) Adsorbed in Mesoporous Silicas Modified with Sulfonated Phenethyl Group

Minoru Sohmiya,[†] Yoshiyuki Sugahara,[‡] and Makoto Ogawa*[,†,§]

Graduate School of Science and Engineering, Waseda University, Nishiwaseda 1-6-1, Shinjuku-ku, Tokyo 169-8050, Japan, Department of Applied Chemistry, Waseda University, Ohkubo 3-4-1, Shinjuku-ku, Tokyo 169-8555, Japan, and Department of Earth Sciences, Waseda University, Nishiwaseda 1-6-1, Shinjuku-ku, Tokyo 169-8050, Japan

Received: July 22, 2006; In Final Form: May 23, 2007

The adsorption of tris(2,2′-bipyridine)ruthenium(II) ($[Ru(bpy)_3]^{2+}$) complex cation into modified mesoporous silicas was investigated. In order to immobilize $[Ru(bpy)_3]^{2+}$, the mesopore surface was modified with sulfonic acid groups by the reactions between MCM-41 and phenethyl(dichloro)methylsilane and the subsequent sulfonation of the attached phenethyl groups with chlorosulfonic acid. The modified mesoporous silicas effectively adsorbed $[Ru(bpy)_3]^{2+}$ from ethanol solution. It was thought that the effective adsorption was the cause of the cooperative effects of the electrostatic interactions between $[Ru(bpy)_3]^{2+}$ cation and sulfonic acid group and the interactions between the phenyl rings on the mesopore surface and the bipyridine rings of the complex. The variation of the position and the intensity of the luminescence of $[Ru(bpy)_3]^{2+}$ suggested that the average distance between the adjacent $[Ru(bpy)_3]^{2+}$ changed with the loading amounts.

Introduction

The immobilization of guest species into porous inorganic solids has extensively been investigated to construct functional inorganic−organic supramolecular materials.[1,2] The states of functional groups on the surface must affect the physicochemical properties of the resulting hybrid materials. The controlled adsorptive properties of surface modified silica gels[3] and layered silicates[4] and long-lived charge separated states in a sol−gel matrix[5] are known examples to show the merits of the immobilization of functional units in a controlled manner. Host−guest and guest−guest interactions are factors to control the properties, so that systematic study on the preparation and characterization of hybrid materials of various compositions and nanostructures are worth conducting to optimize the performance of the resulting hybrid materials.

After the discovery of mesoporous silicas prepared by the cooperative organization of surfactant and inorganic species, the synthesis, characterization, and applications of the supramolecular templated mesostructured materials have extensively been investigated. Mesoporous silicas (MCM-41, FSM-18, SBA-15, etc.) possess such attractive features as well-defined and controllable pore sizes (in the range of 2 to several hundreds of nm), large surface area, and reactive surfaces for the guest organization.[6] Accordingly, the immobilization of guest species in mesoporous silicas has extensively been investigated to construct functional inorganic−organic supramolecular materials for such applications as catalyst and optical material.[6−9] Although the spatial distribution of functional units as well as their mobility are the factors to control the properties of the resulting hybrid materials, they are yet to be investigated. Here we report the adsorption of tris(2,2′-bipyridine)ruthenium(II) complex cation (abbreviated as $[Ru(bpy)_3]^{2+}$, which is one of the photoactive species studied most extensively because of its unique combination of chemical stability, capability of photosensitizing redox reactions, and photophysical properties[10]) onto organically modified mesoporous silicas. We have already reported that the luminescence intensity of $[Ru(bpy)_3]^{2+}$ adsorbed onto a mesoporous silica, FSM-18, substantially decreased upon dehydration and increased upon hydration.[11] The luminescence intensity changes reversibly, indicating that the adsorbed $[Ru(bpy)_3]^{2+}$ cations aggregate to cause self-quenching in the dehydrated state while those are dispersed molecularly in the hydrated state. In addition to the luminescence, vapochromic (change spectroscopic characteristics upon the exposure to a certain vapor) properties and catalytic properties of $[Ru(bpy)_3]^{2+}$ doped mesoporous silicas have also been reported previously.[11−15] In our separate study on the adsorption of tris(8-hydroxyquinoline)aluminum(III) (Alq_3) onto a mesoporous silica with the pore size of 3.1 nm, the luminescence altered with respect to the amount of adsorbed Alq_3.[16] Thus, the effects of the adsorbed amount of $[Ru(bpy)_3]^{2+}$ on the properties of the hybrids are worth investigating to understand the states of the adsorbed $[Ru(bpy)_3]^{2+}$ in the mesopore. The effects of pore size on the states of the $[Ru(bpy)_3]^{2+}$ are also worth investigating in order to highlight the characteristic features (uniform and controllable pore size) of surfactant templated mesoporous silicas. Though the immobilization of photoactive species onto mesoporous silicas have been reported extensively,[9] the effects of pore size on the photophysical and photochemical properties have not been examined.

In our preliminary communication, we have reported that surface modification on a mesoporous silica, FSM-18, significantly affected the adsorption behaviors of $[Ru(bpy)_3]^{2+}$.[17] The incorporation of aluminum and sulfonic acid groups into mesoporous silicas resulted in the increased adsorption capacity for $[Ru(bpy)_3]^{2+}$. The amounts of the adsorbed $[Ru(bpy)_3]^{2+}$ are close to the cation exchange capacities determined by the

* Author to whom correspondence should be addressed.
[†] Graduate School of Science and Engineering.
[‡] Department of Applied Chemistry.
[§] Department of Earth Sciences.

10.1021/jp064654r CCC: $37.00
Published on Web 06/30/2007

titration with NaOH, indicating that $[Ru(bpy)_3]^{2+}$ adsorbed by electrostatic interactions with negatively charged sites formed by the surface modifications. In addition to the adsorption capacity, the luminescence characteristics changed by the surface modification. When $[Ru(bpy)_3]^{2+}$ was adsorbed on the FSM-18 modified by the incorporation of aluminum or propylsulfonic acid group, the luminescence intensity of $[Ru(bpy)_3]^{2+}$ changed dramatically and reversibly upon hydration/dehydration as a result of the aggregation/deaggregation of the $[Ru(bpy)_3]^{2+}$ in the mesopore. On the other hand, the luminescence of $[Ru(bpy)_3]^{2+}$ did not show such vapochromic behavior when FSM-18 modified with phenethylsulfonic acid group was used. The interactions between $[Ru(bpy)_3]^{2+}$ and phenethylsulfonic acid group are so strong that $[Ru(bpy)_3]^{2+}$ is fixed even in the dehydrated state and the redistribution of adsorbed $Ru(bpy)_3]^{2+}$ is less plausible. The controlled adsorption capacity and the variation of the stimuli responsive spectroscopic characteristics are worth further investigating for the applications of dye-doped mesoporous silicas to sensors and reaction media for photochemical reactions. In this paper, we report the adsorption of $[Ru(bpy)_3]^{2+}$ on MCM-41 modified with phenethylsulfonic acid group. The variation of the luminescence characteristics were investigated as a function of the loading amounts as well as the pore size to define the spatial distribution of $[Ru(bpy)_3]^{2+}$ in the mesopore.

Experimental Section

Materials. Tetramethylammonium hydroxide(abbreviated as TMAOH), dodecyl and hexadecyltrimethylammonium bromide were obtained from Tokyo Kasei Kogyo Co., Ltd. Fumed silica (particle size = 7 nm, surface area = 390 ± 40 m^2 g^{-1}) and $[Ru(bpy)_3]^{2+}$ dichloride hexahydrate were obtained from Sigma-Aldrich Co. Phenethyl(dichloro)methylsilane was obtained from Azumax Co. Dehydrated acetonitrile, dehydrated chloroform, and chlorosulfuric acid were obtained from Kanto Chemical Co. All chemicals were used without further purification.

Sample Preparation. Mesoporous silicas were hydrothermally synthesized by the method described by Mokaya[18] from fumed silica, surfactant, TMAOH, and water at the molar ratio of 1:0.25:0.2:40 (SiO_2:surfactant:TMAOH:H_2O). The mixture was sealed in a Teflon lined autoclave and allowed to react at 423 K for 48 h. The products were washed with deionized water until bromide free and dried under reduced pressure. The as-synthesized mesoporous silicas were dried under reduced pressure at 60 °C for 3 h and then allowed to react with phenethyl(dichloro)methylsilane in dehydrated acetonitrile by refluxing under nitrogen flow for 18 h to attach phenethyl groups on the mesopore surface. The weight ratio is 1:19.6:5.6 (as-synthesized mesoporous silica:dehydrated acetonitrile:phenethyl-(dichloro)methylsilane). The products were washed with acetonitrile for 1 day using Soxhlet's extractor and dried under air at 100 °C for 1 day. The sulfonation was conducted by treating the silylated mesoporous silicas dried under reduced pressure at 120 °C for 3 h and then dispersed in dehydrated chloroform, with slow addition of chlorosulfonic acid under nitrogen flow and refluxed for 22 h at the weight ratio of 1:148.4:35.7(silylated mesoporous silica:dried chloroform:chlorosulfonic acid). The products were washed with chloroform, acetone and deionized water and dried under reduced pressure. The products were designated as SPh−MPS-*n*, where *n* denotes the carbon number of the alkyl chain in the template.

The adsorption of $[Ru(bpy)_3]^{2+}$ into the mesoporous silicas was conducted by the reaction between mesoporous silicas with ethanol solutions of $[Ru(bpy)_3]^{2+}$ dichloride hexahydrate (2.5−1 mmol/L) at room temperature for 1 day and subsequent washing with ethanol. The $[Ru(bpy)_3]^{2+}$ adsorbed samples were characterized after the drying under reduced pressure.

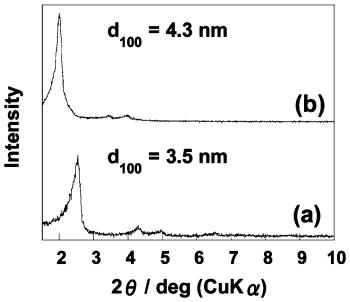

Figure 1. X-ray powder diffraction patterns of SPh−MPS-12 (a) and SPh−MPS-16 (b).

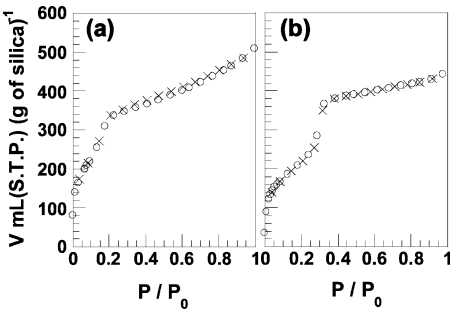

Figure 2. Nitrogen adsorption/desorption isotherms of SPh−MPS-12 (a) and SPh−MPS-16 (b); (circle) adsorption and (cross) desorption.

Characterization. X-ray powder diffraction patterns were obtained on a Rigaku Rad IB diffractometer using monochromatic Cu Kα radiation operated at 40 kV and 20 mA. Solid state ^{29}Si MAS NMR and ^{13}C CP/MAS NMR spectrum was recorded on a JEOL JNM-EX270 spectrometer. CHN analysis was performed on a Perkin-Elmer 2400 II instrument. The nitrogen adsorption/desorption isotherms were measured at 77 K on a BELSORP 28 instrument (BEL Japan, Inc.). Prior to the measurement, the sample was evacuated at 120 °C for 3 h. Visible absorption spectra were recorded on a Shimadzu UV-3100PC spectrophotometer using an integrated sphere. The adsorbed amount of $[Ru(bpy)_3]^{2+}$ was determined by the change in the concentration in ethanol solutions before and after the reactions with SPh−MPSs. The concentration of $[Ru(bpy)_3]^{2+}$ was determined by the change in the absorbance at 452 nm, which is due to MLCT transition of $[Ru(bpy)_3]^{2+}$, using Shimadzu UV-3100PC spectrophotometer. Luminescence spectra were recorded on a Hitachi F-4500 fluorospectrophotometer in the range of 500−800 nm with the excitation at 450 nm. The bandwidth of the excitation wavelength and the emission wavelength was 5 nm.

Results and Discussion

The formation of organically modified mesoporous silicas was confirmed by the X-ray diffraction patterns and the nitrogen adsorption/desorption isotherms. The X-ray diffraction patterns of SPh−MPS-12 and -16 exhibit four lines, which are ascribable to the (100), (110), (200), and (210) reflections of hexagonal mesostructures typical to MCM-41. The nitrogen adsorption/desorption isotherms are shown in Figure 2, which are classified as type IV showing the presence of mesopore. SPh−MPS-12 and -16 possess BET surface area of ca. 960 and 760 m^2 (g of silica)$^{-1}$ with the average pore diameter of 2.2 and 3.0 nm, respectively, as determined from the nitrogen adsorption isotherms by BJH method.[19] The attachment of the phenethyl

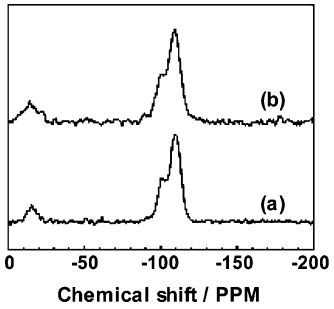

Figure 3. ^{29}Si MAS NMR spectra of SPh−MPS-12 (a) and SPh−MPS-16 (b).

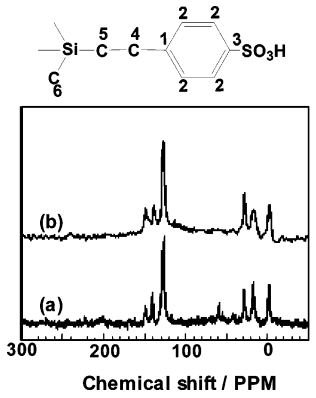

Figure 4. ^{13}C CP/MAS NMR spectra of SPh−MPS-12 (a) and SPh−MPS-16 (b).

sulfonic group on the mesopore surface was evidenced by elemental analyses and NMR spectroscopy. The ^{29}Si MAS NMR spectra of SPh−MPS-12 and -16 are shown in Figure 3. SPh−MPS-12 and -16 shows four peaks at ca. −110, −102, −90, and −16 ppm corresponding to Q^4 ($(SiO)_4Si$), Q^3 ($(SiO)_3Si(OH)$), Q^2 ($(SiO)_2Si(OH)_2$), and the silicon nuclei of the organosilyl grafted species. Both samples showing the peaks which were attributed to Q^3 or Q^2, indicating that some silanol groups exist on the mesopore surface. The ^{13}C CP/MAS NMR spectra of SPh−MPS-12 and -16 are shown in Figure 4. SPh−MPS-12 shows signals at 17.5 and 28.6 ppm corresponding to the methylene C^5 and C^4 carbons and a signal at −1.5 ppm from methyl C^6 carbon. The signals occurring at 149.0 ppm, 140.4, 128.9, and 126.4 ppm were attributed to the aromatic carbons. SPh−MPS-16 shows peaks at 148.4, 138.3, 127.0, 27.9, 16.6, and −2.0 ppm, which were attributed to aromatic hydrocarbon attached with sulfonic acid group. These results are consistent with those reported for silica gel system[20] as well as surfactant templated mesoporous silica systems,[13,21−23] where sulfonic acid group was attached to the phenethyl groups on the pore surface, confirming the successful formation of the sulfonated phenethyl groups on the mesopore surface. The chemical composition of SPh−MPS-12 and -16 are summarized in Table 1. From the carbon content of SPh−MPSs, the amount of the attached organic groups were determined to be 1.8 mmol (g of silica)$^{-1}$, which corresponds to 1.1 and 1.4 groups/nm^2. Assuming that the attached functional groups distribute homogeneously on the mesopore surface, the average distance between adjacent sulfonated phenethyl groups was estimated to be 1.1 and 0.93 nm for SPh−MPS-12 and -16, respectively.

By the reaction of SPh−MPSs with $[Ru(bpy)_3]^{2+}$ chloride ethanol solutions, orange solids were obtained. The adsorption isotherms of $[Ru(bpy)_3]^{2+}$ onto SPh−MPSs are shown in Figure 5. The isotherms are type H according to the Giles and Smith

TABLE 1: Properties of SPh−MPSs

sample	BET surface area (m^2 (g of silica)$^{-1}$)	BJH pore size (nm)	pore volume[a] (mL (g of silica)$^{-1}$)
SPh−MPS-12	960	2.2	0.53
SPh−MPS-16	750	3.0	0.57

	amount of sulfonated phenethyl groups		
sample	(mmol (g of silica)$^{-1}$)[b]	(groups/nm^2)[c]	(nm)[d]
SPh−MPS-12	1.8	1.1	0.93
SPh−MPS-16	1.8	1.4	1.1

[a] Calculated from BET surface area and BJH pore size. [b] The amount of sulfonated phenethyl groups are calculated from carbon content of SPh−MPSs. [c] Calculated from carbon content and BET surface area. [d] Calculated from carbon contents, BET surface area and BJH pore size.

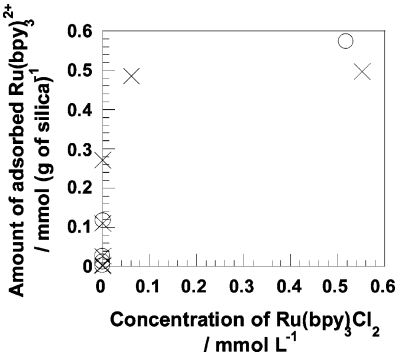

Figure 5. The adsorption isotherms of $[Ru(bpy)_3]^{2+}$ on SPh−MPS-12 (cross) and SPh−MPS-16 (circle).

classification,[24] indicating the strong adsorbent−adsorbate interactions. It was reported that the surface modification of mesopore surface with amino group resulted in the effective adsorption of an anionic porphyrine.[25] The attachment of functional group on the mesopore was also conducted to immobilize a rare earth complex.[26] Thus, organically modified mesoporous silicas are worth investigating as hosts of dyes. The X-ray diffraction patterns of the products (data not shown) indicated that the mesostructure of SPh−MPSs did not change after the adsorption of $[Ru(bpy)_3]^{2+}$. Considering the adsorption isotherms, the controlled amount of $[Ru(bpy)_3]^{2+}$ can be adsorbed in the mesopore by simply changing the added amounts of $[Ru(bpy)_3]^{2+}$ with retaining the mesostructures. The maximum amount of $[Ru(bpy)_3]^{2+}$ was ca. 0.6 mmol (g of silica)$^{-1}$, irrespective of the pore size. The amount is 2/3 (considering the $[Ru(bpy)_3]^{2+}$ as bidentate) of the amount of attached sulfophenethyl group (1.8 mmol (g of silica)$^{-1}$ for SPh−MPS-12 and -16). The adsorption capacity was thought to be caused by the geometrical constraints as well as the imcomplete sulfonation. Hereafter, the samples containing different amounts of $[Ru(bpy)_3]^{2+}$ are evaluated.

In the visible absorption spectra of the products, the absorption band ascribable to the "metal-to-ligand charge transfer" (MLCT) band[10] of $[Ru(bpy)_3]^{2+}$ was observed at around 454 nm irrespective of the loading amount. Figures 6 and 7 show the photoluminescence spectra, where excitation wavelength was 450 nm, of $[Ru(bpy)_3]^{2+}$ in SPh−MPS-12 and -16, respectively. The luminescence due to the MLCT transition of $[Ru(bpy)_3]^{2+}$ was observed at around 600 nm for all the products. The luminescence maxima were shifted toward longer wavelength region (from 585 to 600 nm) with the increase in the adsorbed $[Ru(bpy)_3]^{2+}$ amount. The variation of the luminescence maxima as a function of the amounts of adsorbed $[Ru(bpy)_3]^{2+}$ is summarized in Figure 8.

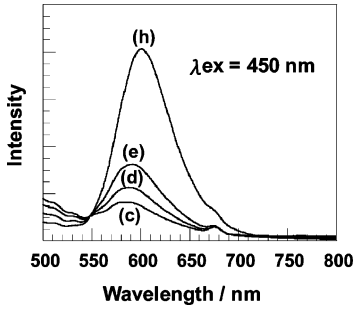

Figure 6. Photoluminescence spectra of the $[Ru(bpy)_3]^{2+}$ adsorbed on SPh−MPS-12. The amount of adsorbed $[Ru(bpy)_3]^{2+}$ are (a) 4.5, (b) 27, (c) 110, and (d) 497 μmol (g of silica)$^{-1}$.

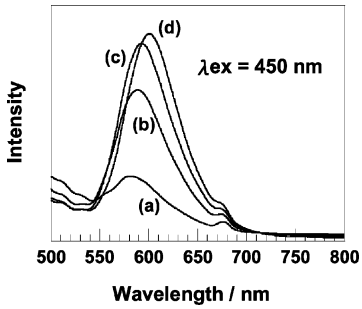

Figure 7. Photoluminescence spectra of the $[Ru(bpy)_3]^{2+}$ adsorbed on SPh−MPS-16. The amount of adsorbed $[Ru(bpy)_3]^{2+}$ are (a) 2.4, (b) 27, (c) 117, and (d) 575 μmol (g of silica)$^{-1}$.

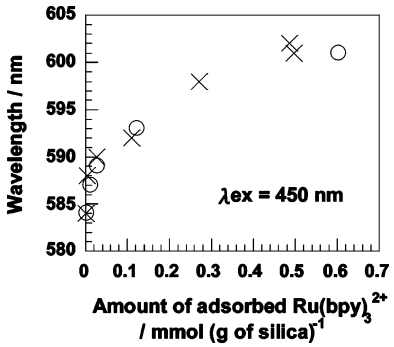

Figure 8. The relationship between the luminescence maxima and the $[Ru(bpy)_3]^{2+}$ adsorbed on SPh−MPS-12(cross) and SPh−MPS-16-(circle).

The immobilization of $[Ru(bpy)_3]^{2+}$ and analogous complexes on zeolites has been investigated so far for the catalytic applications and controlled photoinduced electron transfer by separating donor and acceptor in and on zeolite structures.[27,28] It has been reported that the MLCT luminescence of $[Ru(bpy)_3]^{2+}$ shifts by the complexation with zeolites, reflecting the host−guest interactions. The effects of the hydration on the luminescence wavelength was also reported for the $[Ru(bpy)_3]^{2+}$−zeolite Y system.[28e] Luminescence shifts of MLCT luminescence of the $[Ru(bpy)_3]^{2+}$ have been observed in various heterogeneous systems.[27−30] Wheeler and Thomas observed a luminescence blue shift upon the adsorption of $[Ru(bpy)_3]^{2+}$ on colloidal silica.[29] Blue shifts of the $[Ru(bpy)_3]^{2+}$ luminescence maxima have also been observed in silica and aluminosilica gels through sol-to-gel conversion and gel aging and drying.[30] It was hypothesized that an increased possibility for relaxation in a more fluid state caused the spectral shifts.

In the present system, the luminescence maxima were shifted toward longer wavelength region (from 585 to 600 nm) with the increase in the adsorbed $[Ru(bpy)_3]^{2+}$ amount. These results suggest that the intermolecular interactions between adjacent

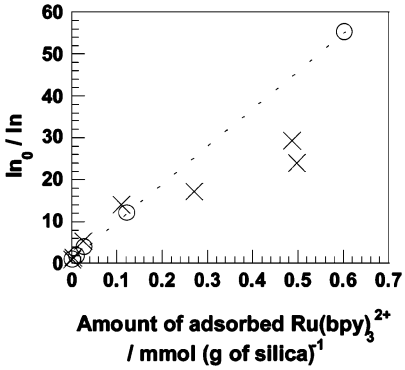

Figure 9. Quasi Stern−Volmer plot of the $[Ru(bpy)_3]^{2+}$ adsorbed on SPh−MPS-12(cross) and SPh−MPS-16(circle).

$[Ru(bpy)_3]^{2+}$ complex cation became dominant with the increase in the $[Ru(bpy)_3]^{2+}$ loading. Similar spectral shift reflecting the proximity has been observed for the $[Ru(bpy)_3]^{2+}$ adsorbed on a layered zirconium phosphate sulfophenylphosphonate,[31] montmorillonite,[32] and polymer-swelling mica intercalation compounds.[33] Since the luminescence maxima changed gradually with the $[Ru(bpy)_3]^{2+}$ loading, the average separation between adjacent $[Ru(bpy)_3]^{2+}$ became smaller and/or the contribution of $[Ru(bpy)_3]^{2+}$ aggregation became dominant with the increase in the $[Ru(bpy)_3]^{2+}$ loading. The relative luminescence intensity decreased with the increase of the $[Ru(bpy)_3]^{2+}$ loading, supporting the idea on the spatial distribution.

Figure 9 shows the quasi Stern−Volmer plot for the luminescence intensity of $[Ru(bpy)_3]^{2+}$ in SPh−MPS-12 and -16. The plots show that the relative luminescence intensity of the complex adsorbed onto SPh−MPSs decreased with the increase of the adsorbed amount of $[Ru(bpy)_3]^{2+}$. There is a linear relationship between the amount of $[Ru(bpy)_3]^{2+}$ and the relative luminescence intensity in the quasi Stern−Volmer plot for SPh−MPS-16 system, indicating that the possibility of luminescence self-quenching increases at higher $[Ru(bpy)_3]^{2+}$ loading. This fact confirms the above discussion on the separation of adjacent $[Ru(bpy)_3]^{2+}$ was controlled by the loading amounts. On the other hand, the relationship is more complicated for SPh−MPS-12 system as seen in Figure 9.

The variation of the luminescence maxima was governed by the loading amount as shown in Figure 8, while the pore size affected the quasi Stern−Volmer plot. Though the factors responsible for the deviation from linear relationship observed for SPh−MPS-12 are not confirmed at present, the smaller pore size of SPh−MPS-12 (2.2 nm) may be concerned. At the higher loading level, the intermolecular separation between adjacent complex in the cross section is not negligible when the diameter of the cylindrical pore became smaller to affect the luminescence self-quenching. Further study on the luminescence intensity variation using mesoporous silicas with different pore sizes is worth conducting to define and to design the spatial distribution of the adsorbed $[Ru(bpy)_3]^{2+}$ more precisely. The pore size effect in the quasi Stern−Volmer plot was seen at the higher loading level (>0.3 mmol ((g of silica)$^{-1}$). As mentioned previously, the amount of organosilyl group (1.8 mmol (g of silica)$^{-1}$ for SPh−MPS-12 and -16, which correspond to the average distance between adjacent sulfonated phenethyl groups of 1.1 and 0.93 nm for SPh−MPS-12 and -16, respectively) was very high in the present system. The residual sulfonated phenethyl group may affect the spatial distribution of the $[Ru(bpy)_3]^{2+}$ as well as the photophysics of the adsorbed $[Ru(bpy)_3]^{2+}$.

TABLE 2: Properties of $[Ru(bpy)_3]^{2+}$ Adsorbed on SPh−MPSs

sample SPh−MPS	amount of the adsorbed $[Ru(bpy)_3]^{2+}$ (mmol (g of silica)$^{-1}$)	the volume occupied by the $[Ru(bpy)_3]^{2+}$ (mL)[a]	average distance between $[Ru(bpy)_3]^{2+}$ (nm)[b]
-12(a)	0.0012	0.0006	146.47
(b)	0.0045	0.0023	37.20
(c)	0.027	0.0138	6.33
(d)	0.110	0.0570	1.53
(e)	0.271	0.140	0.62
(f)	0.486	0.252	0.35
(g)	0.497	0.257	0.34
-16(a)	0.0024	0.0013	54.73
(b)	0.011	0.0059	11.70
(c)	0.027	0.0141	4.88
(d)	0.117	0.0606	1.14
(e)	0.575	0.298	0.23

[a] Calculated from the amount of the adsorbed $[Ru(bpy)_3]^{2+}$ and the volume occupied by one $[Ru(bpy)_3]^{2+}$ molecule. The volume was calculated from the assumption that $[Ru(bpy)_3]^{2+}$ is sphere, and its diameter is 1.18 nm. [b] Calculated from the amount of the adsorbed $[Ru(bpy)_3]^{2+}$, BET surface area and BJH pore size.

The volume occupied by the adsorbed $[Ru(bpy)_3]^{2+}$ was determined from the BET surface area, pore geometry and the adsorbed $[Ru(bpy)_3]^{2+}$ amount as summarized in Table 2. At the loading level of 0.27 mmol (g of silica)$^{-1}$ adsorbed on SPh−MPS-12, the volume occupied by $[Ru(bpy)_3]^{2+}$ was estimated to be ca. 0.14 mL (g of silica)$^{-1}$. Since the pore volume of SPh−MPS-12 was 0.53 mL (g of silica)$^{-1}$ as determined from the nitrogen adsorption isotherm, it seems that the concentration quenching of the luminescence cannot be avoided at such high concentration loadings. The concentration quenching was observed when the loading level was very low (below 0.05 mmol (g of silica)$^{-1}$). At such loading level, the luminescence intensity changed dramatically while the luminescence maxima did not depend apparently on the loading.(Figure 8) This observation suggests that a portion of the adsorbed $[Ru(bpy)_3]^{2+}$ aggregated to cause self-quenching (clustering) at such low loading level (below 0.05 mmol (g of silica)$^{-1}$). The distance dependent changes in the luminescence characteristics have been reported for such flexible systems as two-dimensional expandable spaces of layered materials[31−33] and polymer.[34] Porous Vycor Glass has also been used to immobilize $[Ru(bpy)_3]^{2+}$ with controlled surface coverage.[35] If compared with those systems, mesoporous silicas provide unique low dimensionally defined reaction media for the guest organization.

The organic modification of mesoporous silica with sulfonated phenethyl group resulted in the successful attachment of acidic sites on the mesopore surface as evidenced by the adsorption of the cationic complex ion. The amount of the complex was controlled by the added amounts of $[Ru(bpy)_3]^{2+}$ in the present study. The amount of sulfonated phenethyl group is also controllable by changing the amount of silane coupling reagent used in the surface modification. The surface modification is possible for the mesoporous silicas with different pore size. Thus, there are so many options of nanospaces through the modification of mesoporous silicas. The photochemistry and photophysics of cationic dyes on the modified mesoporous silicas are worth further investigating toward controlled photochemical reactions including photoinduced electron transfer affected by the guest−guest interactions as well as the unique spatial distribution confined in a low dimensional nano space. In order to simplify the nanostructures of the host−guest systems, it should be fruitful to vary the organosilyl groups in the nanospace.

Conclusions

The adsorption of $[Ru(bpy)_3]^{2+}$ onto mesoporous silicas modified with sulfonated phenethyl groups from ethanol solution was investigated. The sulfonated phenethyl groups was successfully attached on the mesopore surface by the silylation of silica-surfactant mesostructured materials with phenethyl(dichloro)methylsilane and the subsequent sulfonation of the attached phenethyl groups with chlorosulfonic acid. The sulfonated phenethyl group covalently bound to the mesopore surface is effective to immobilize $[Ru(bpy)_3]^{2+}$. The average distance between the adjacent $[Ru(bpy)_3]^{2+}$ varied depending upon the loading level as suggested by the variation of the luminescence maxima and the intensity.

Acknowledgment. This work was financially supported by a Grant-in-Aid for Scientific Research on Priority Areas (417) from the Ministry of Education, Culture, Sports, Science and Technology (MEXT) of the Japanese Government, Tokuyama Science and Technology Foundation, CREST, JST, and Waseda University (Waseda University Fund for Special Project Research, 2005B-073, 2005B-074).

References and Notes

(1) Ozin, J. A. *Adv. Mater.* **1992**, *4*, 612.
(2) Ogawa, M.; Kuroda, K. *Chem. Rev.* **1995**, *95*, 399.
(3) Wirth, M. J.; Fairbank, R. W. P.; Fatunmbi, H. O. *Science* **1997**, *275*, 44.
(4) Ogawa, M.; Okutomo, S.; Kuroda, K. *J. Am. Chem. Soc.* **1998**, *120*, 7361.
(5) Slama-Schwok, A.; Ottolenghi, M.; Avnir, D. *Nature* **1992**, *355*, 240.
(6) Raman, N. K.; Anderson, M. T.; Brinker, C. J. *Chem. Mater.* **1996**, *8*, 1682.
(7) Ciesla, U.; Schüth, F. *Microporous Mesoporous Mater.* **1999**, *27*, 131.
(8) (a) Moller, K.; Bein, T. *Chem. Mater.* **1998**, *10*, 2950. (b) Corma, A. *Chem. Rev.* **1997**, *97*, 2373.
(9) (a) Scott, B. J.; Wirnsberger, G.; Stucky, G. D. *Chem. Mater.* **2001**, *13*, 3140. (b) Ogawa, M. *J. Photochem. Photobiol., C* **2002**, *3*, 129.
(10) Kalyanasundaram, K. *Photochemistry of Polypyridine and Porphyrin Complexes*, Academic Press: London, 1992.
(11) (a) Ogawa, M.; Nakamura, T.; Mori, J.; Kuroda, K. *J. Phys. Chem. B* **2000**, *104*, 8554. (b) Ogawa, M.; Nakamura, T.; Mori, J.; Kuroda, K. *Microporous Mesoporous Mater.* **2001**, *48*, 159.
(12) Fang, M.; Wang, Y.; Zhang, P.; Li, S.; Xu, R. *J. Lumin.* **2000**, *91*, 67.
(13) Liu, C.; Te, X.; Wu, W. *Catal. Lett.* **1996**, *36*, 263.
(14) (a) Kim, S.-S.; Zhang, W.; Pinnavaia, T. J. *Catal. Lett.* **1997**, *43*, 149. (b) Fujishima, K.; Fukuoka, A.; Ichikawa, M.; Yamagishi, A.; Inagaki, S.; Fukushima, Y.; Ichikawa, M. *J. Mol. Catal. A: Chem.* **2001**, *166*, 211.
(15) Villemure, G.; Pinnavaia, T. J. *Chem. Mater.* **1999**, *11*, 789.
(16) Tagaya, M.; Ogawa, M. *Chem. Lett.* **2006**, *35*, 108.
(17) Ogawa, M.; Nakamura, T.; Kuroda, K. *Chem. Lett.* **2002**, 632.
(18) Mokaya, R. *J. Phys. Chem. B* **2000**, *104*, 8279.
(19) Barrett, E. P.; Joyner, L. G.; Halenda, P. P. *J. Am. Chem. Soc.* **1951**, *73*, 373.
(20) Badley, R. D.; Ford, W. T. *J. Org. Chem.* **1989**, *54*, 5437.
(21) Mohino, F.; Diaz, I.; Perez-Pariente, J.; Sastre, E. *Stud. Surf. Sci. Catal.* **2002**, *142*, 1275.
(22) Merelo, J. A.; Stucky, G. D.; van Grieken, R.; Morales, G. *J. Mater. Chem.* **2002**, *12*, 1664.
(23) Herledan-Sem, mer, V.; Dakhlaoui, S.; Guenneau, F.; Haddad, E.; Gedeon, A. *Stud. Surf. Sci. Catal.* **2004**, *154*, 1519.
(24) Giles, C. H.; Smith, D. *J. Colloid Interface Sci.* **1974**, *47*, 3.
(25) Xu, W.; Guo, H.; Akins, D. L. *J. Phys. Chem. B* **2001**, *105*, 1543.
(26) Xu, Q. H.; Li, L. S.; Li, B.; Yu, J. H.; Xu, R. R. *Microporous Mesoporous Mater.* **2000**, *38*, 351.
(27) (a) DeWilde, W.; Peeters, G.; Lunsford, J. H. *J. Phys. Chem.* **1980**, *84*, 874. (b) Quayle, W. H.; Lunsford, J. H. *Inorg. Chem.* **1982**, *21*, 97. (c) Lunsford, J. H. *Rev. Inorg. Chem.* **1987**, *9*, 1. (d) Dutta, P. K.; Incavo, J. A. *J. Phys. Chem.* **1987**, *91*, 4443. (e) Incavo, J. A.; Dutta, P. K. *J. Phys. Chem.* **1990**, *94*, 3075. (f) Kim, Y. I.; Mallouk, T. E. *J. Phys. Chem.* **1992**, *96*, 2879. (g) Turbeville, W.; Robins, D. S.; Dutta, P. K. *J. Phys. Chem.* **1992**, *96*, 5024. (h) Bhuiyan, A. A.; Kincaid, J. R. *Inorg. Chem.* **1999**, *38*, 4759.

(28) Maruszewski, K.; Strommen, D. P.; Kincaid, J. R. *J. Am. Chem. Soc.* **1993**, *115*, 8345.
(29) Wheeler, J.; Thomas, J. K. *J. Phys. Chem.* **1982**, *86*, 4540.
(30) Innocenzi, P.; Kozuka, H.; Yoko, T. *J. Phys. Chem. B* **1997**, *101*, 2285. Matsui, K.; Sasaki, K.; Takahashi, N. *Langmuir* **1991**, *7*, 2866.
(31) (a) Colón, J. L.; Yang, C.-Y.; Clearfield, A.; Martin, C. R. *J. Phys. Chem.* **1988**, *92*, 5777. (b) Colón, J. L.; Yang, C.-Y.; Clearfield, A.; Martin, C. R. *J. Phys. Chem.* **1990**, *94*, 874.
(32) Schoonheydt, R. A.; de Pauw, P.; Vliers, D.; de Schryver, F. C. *J. Phys. Chem*. **1984**, *88*, 5113.
(33) Ogawa, M.; Tsujimura, M.; Kuroda, K. *Langmuir* **2000**, *16*, 4202.
(34) Nagai, K.; Takamiya, N.; Kaneko, M. *J. Photochem. Photobiol., A* **1994**, *84*, 271.
(35) (a) Shi, W.; Wolfgang, S.; Gafney, H. D. *J. Phys. Chem.* **1985**, *89*, 974. (b) Gafney, H. D. *Coord. Chem. Rev.* **1990**, *104*, 113.